C. R. Physique 19 (2018) 672–687

Contents lists available at ScienceDirect

Comptes Rendus Physique

www.sciencedirect.com

New trends in metallic alloys / Alliages métalliques : nouvelles tendances

Recent advances in the metallurgy of aluminium alloys. Part I: Solidification and casting

Développements récents en métallurgie des alliages d'aluminium. Première partie : coulée et solidification

Philippe Jarry [a,*], Michel Rappaz [b]

[a] *Constellium Technology Center, Parc économique Centr'Alp, 725, rue Aristide-Bergès, CS 10027, 38341 Voreppe cedex, France*
[b] *École polytechnique fédérale de Lausanne, Institute of Materials, Station 12, 1015 Lausanne, Switzerland*

ARTICLE INFO

Article history:
Available online 3 October 2018

Keywords:
Aluminium
Solidification
Casting

Mots-clés :
Aluminium
Solidification
Coulée

ABSTRACT

The goal of these review papers is to summarize the recent advances in the metallurgy of aluminium alloys and from this analysis, to try to outline future developments in this field. Part I deals with the transformation of aluminium alloys from the liquid to the solid state, while Part II will focus on solid-state transformations. These papers are by no means exhaustive since the literature is very abundant, but the authors wish to give a personal view of what they think are the most relevant scientific contributions that can impact future technological developments.

RÉSUMÉ

L'objet de ces articles de synthèse est de résumer les progrès récents de la métallurgie des alliages d'aluminium et, en partant de cette analyse, d'essayer de définir les développements futurs dans ce domaine. La partie I traite de la transformation des alliages d'aluminium de l'état liquide à l'état solide, tandis que la partie II se concentre sur les transformations à l'état solide. Ces articles ne sont en aucun cas exhaustifs, car la littérature est très abondante, mais les auteurs souhaitent donner un point de vue personnel sur ce qu'ils pensent être les contributions scientifiques les plus pertinentes pouvant influer sur les développements technologiques futurs.

* Corresponding author.
E-mail address: philippe.jarry@constellium.com (P. Jarry).

https://doi.org/10.1016/j.crhy.2018.09.003
1631-0705/

1. Introduction

The metallurgical studies of the transformations of aluminium alloys from a liquid to a solid state are driven by industrial needs. Before going into the depth of the recent scientific developments in that field, it is useful to have a clear representation of the driving forces at work for process evolution in a metallurgical company. There are three kinds of requirements.

- *Prescriptive requirements*, or constraints, whether internal (existing assets, investment choice...) or external (regulations), which apply to a given metallurgical company. The never-ending path toward reliability and robustness of a production process, including automation, is indeed a driving force for a company endlessly striving to standardize its processes as excellence must be reproduced every day! Although this could be considered as having little impact on the evolution of metallurgy, this stimulates some kind of knowledge improvement. In order to reduce scatter of the production and improve productivity, it is necessary to understand the sources of scatter. Control of *process* variability stimulates both the use of sensor/actuator systems and basic – mostly thermal – modelling of casting lines. Control of *materials* variability sets off basic solidification studies relying more on statistical evidence than on in-depth understanding. It is in particular necessary to decide what to require in terms of specification evolution imposed to master alloys, grain refiners, modifiers, etc.
- *Organic requirements*, that is, what commands and justifies process evolution in relation with explicit customer specifications and implicit market trends. This evolution axis is organic in the sense that it leads to considering the production schedule as a whole, with emphasis on the heredity of the solidification structure in the downstream metallurgical transformations. For our purpose, this starts right from the liquid structure (see §2.4): the icosahedral short-range order (ISRO) is influenced by transition metals and is reflected in the crystal structure of many intermetallic phases that are quasicrystals approximants. This has an impact also on nucleation and growth. In aluminium alloys, solute elements are primarily of substitutional type and thus their diffusion in the liquid state is at least three orders of magnitude faster than in the solid. Therefore, the casting stage shall be considered as the first metallurgical step toward the end product specifications. Besides, what is obtained at the solidification stage may not be reversible in the solid state unless the down gauging is strong enough to decrease the diffusion scales accordingly. The genes of this heredity are mostly borne by micro- and macro-segregations and consideration thereof leads to devising alloy design rules. The spatial distribution, size, morphology, and nature of secondary phases formed during solidification are primarily controlled by the local solidification conditions as well as by the grain size and morphology of the primary phase. Solidification and casting engineering requires the construction of adapted mock-ups or models, which have been and still are the basis of the engineer's iconic language [1]. This effort is very demanding in terms of thorough knowledge of the physical mechanisms involved and has been in recent years fertilised by two imaging means, virtual and real. First, the fantastic development of *numerical modelling*, which gives insight to, and guides optimisation of, casting parameters in relation with solidification structure and end-product properties. Micro- and macro-scales are coupled by transport equations governing fluid flow, transport and deformation of the solid phase. The influence of convection on grain fragmentation and growth of primary dendrites is another important parameter. Capillary forces at free liquid surfaces may also play a crucial role at the scale of the melt when its dimensions are small, e.g., Marangoni thermal- or solutal-convection in the melt pool in laser melting or welding. The other visualisation technique is by means of *quantitative metallography*. Orientation imaging of the microstructure, based on Electron Back-Scattered Diffraction (EBSD), has demonstrated its power over the past twenty-five years not only in the solid state but also in solidification. Thanks to the transparency of aluminium to X-rays and the development of *large instruments* such as synchrotrons, *in situ* observations provide insight into otherwise opaque crystallising melts. Lab-scale transmission X-ray setups have also proven useful to visualise solidification mechanisms. They allow studying the effect of grain refining strategies, solidification parameters and possibly external fields on the resulting structures.
- *Innovative driving forces*, or can we do things differently? We know of many casting processes, especially rapid solidification processes such as melt spinning, which never quite succeeded in industrial applications, mainly because they did not meet the organic requirements mentioned above, *viz.* customer specifications and implicit market needs. Recently, the emergence of additive manufacturing, and in particular, for aluminium alloys, of Selective Laser Melting (SLM) of powder beds, leads us to revisiting rapid solidification studies and concepts dating back to the 1990s in a renewed process context with strong implications on alloy design rules (see §5).

This review paper is subdivided as follows. Section 2 summarizes the recent advances in numerical simulation of casting and solidification at various scales, with a particular focus on aluminium alloys. In situ observations of solidification made possible with large-scale (synchrotrons) or lab-scale X-Ray set-ups are summarized in Section 3. Section 4 is dedicated to microstructure selection, considering both nucleation and growth, while Section 5 outlines the needs for the specific development of Al alloys in additive manufacturing, i.e. when the solidification speed can potentially induce non-equilibrium conditions at the solid–liquid interface. Finally, before the conclusion and perspectives, the influence of convection on solidification is approached in Section 6.

2. Panorama of recent numerical modelling progress in the field of casting and solidification of Al alloys

With the fantastic development of computing power and the advances of numerical methods, numerical modelling of solidification and casting processes has been able to address increasingly complex problems, at multiple scales. This section reviews some of these progresses, starting from the macroscopic scale down to the atomistic level, with a focus on aluminium alloys and processes. For readers interested to know more about solidification modelling approaches in general, we refer to two recent short review articles [2,3].

2.1. Multiscale modelling of the DC casting process

By multiscale modelling, it is meant that macroscopic equations governing energy – (most often reduced to heat-), mass-, momentum- and species-conservation are coupled with analytical models describing nucleation, growth and possibly settling of grains [4,5]. Such approaches for equiaxed grains have been made possible by replacing the complex dendritic or globular–dendritic microstructure by the concept of an envelope, whose growth kinetics is given by an analytical model of the growth of the active dendrite branches [6–8]. A local solute balance accounting for the solute concentration field in the vicinity of the envelope allows one to deduce the internal fraction of solid within the grains [9]. These multiscale models have brought very valuable insight into a process such as Direct Chill (DC) casting of Al alloys.

Before grain transport was included in such multiscale models, nucleation was thought to occur more or less uniformly in the whole casting, in a region close to the liquidus isotherm. Accounting for the transport by convection of inoculant particles, of already-formed nuclei as well as of solute elements taught us that nucleation events are limited to a small zone of the DC cast ingot, next to the ingot surface in contact with the mould. This zone acts as a "grain factory" and the uneven distribution of nuclei and solute elements due to convection fundamentally governs subsequent grain growth, and thus the final grain size, across the slab section [10].

Macrosegregation can bring some regions of a casting out of the composition specifications or lead to an unacceptable amount of secondary phases. Unlike microsegregation, which can be "erased" during homogenisation, macrosegregation profiles remain during the whole processing of the alloy. The final macrosegregation pattern in an ingot results from the possibility of a relative movement between the solid and liquid phases, which have different compositions, the solid being leaner (resp. richer) in eutectic (resp. peritectic[1]) solutes than the liquid within the solidification interval. In parallel, the difference between the transport of the liquid and solid phases governs the local supersaturation, and thus the growth rate of the microstructure. These complex mechanisms, which are of primary importance for industrial processes, can only be captured by complex models [11]. Since the pioneering work of Flemings [12], the negative[2] segregation observed at the centre of DC cast ingots can be explained by the shape of the isotherms and of the diverging flow lines compensating for solidification shrinkage [13], while according to the same principle the converging downward flow of eutectic-enriched liquid in the mushy zone, parallel to the front, may create a positive segregation peak at mid-thickness. However, while liquid enrichment in dense solutes (Zn, Cu…) upon cooling contributes to making it denser, the presence of light alloying elements such as Mg or Li creates a discordance between the respective effects of temperature decrease and solute enrichment on the liquid density, causing thermo-solutal convection to appear, with complex consequences on the macrosegregation pattern. Finally, the settling at the sump bottom of heavier grains being leaner in eutectic solute elements [4,14] can reinforce the negative centreline macrosegregation. Settling-induced macrosegregation is much more pronounced for globular-type grains, since dendritic ones tend to be transported with their internal fraction of liquid. Therefore, the way these grains tumble, pack and transport solute with them is an important part of the picture and depends on their morphology, itself dictated by their growth and thus by the local solute content and temperature. Recently, a multi-sphere clumping Discrete Element Method (DEM) approach was employed [15] to predict the solid packing fraction of grains depending upon their degree of sphericity. This opens the way to a better physical description of grain packing in macrosegregation models.

One of the remaining and important challenges of such mesoscopic models is the growth kinetics law describing the evolution of the envelope. While it is fairly well known for small spherical grains and for fully-developed dendritic equiaxed grains, the transition between these two morphologies – like cells in columnar growth – has no simple analytical solution. Inoculated Al alloys fall typically within this transition range since the final grains exhibit a so-called globular–dendritic morphology, i.e. neither globules nor dendrites. This is illustrated in Fig. 1 by plotting R_{g-d} (for a given cooling rate $\dot{T} = 1$ K/s), that is the globular-to-dendritic destabilisation radius predicted according to [16], as a function of the growth restriction coefficient $m(k-1)C_0$ and comparing it with actual grain sizes. The globular-to-dendritic destabilisation radius scales as:

$$R_{g-d} = \left(96 \frac{D_\ell \Gamma_{s\ell} L_f}{m(k-1)C_0 c_p \dot{T}}\right)^{1/3} \tag{1}$$

[1] In Al-based binary systems there are nine peritectic elements (i.e. with partition coefficient > 1), *viz.* Ti, Zr, Hf, V, Nb, Ta, Cr, Mo, W. All the others are eutectic (partition coefficient < 1) or have no solubility in liquid Al.

[2] "Negative" should be understood as "leaner in eutectic elements", but peritectic solutes exhibit the opposite trend.

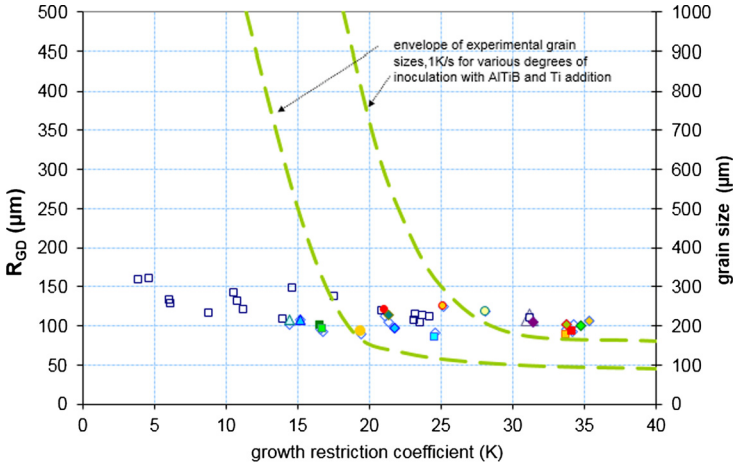

Fig. 1. Comparison between the grain radius for which the globular–dendritic transition is predicted (cloud of points) and the effective experimental grain sizes obtained at the laboratory for one set of cooling and inoculation conditions representative of ingot DC Casting (schematized by its envelop in dashed lines), for various alloys ranked by their "growth restriction coefficient", $m_i(k_i - 1)C_{0i}$.

where m is the liquidus slope, C_0 is the solute content of the bulk liquid, k is the solute partition coefficient, D_ℓ is the diffusion coefficient of the solute in the liquid phase, $\Gamma_{s\ell}$ is the Gibbs–Thomson coefficient accounting for capillarity, and L_f/c_p is the ratio of the latent heat to the specific heat. This figure shows that for alloys with a low coefficient, grains get dendritic before reaching their final size while alloys with a high coefficient reach their final grain size before grain growth fully destabilises, thus remaining globular [17]. Note that for a given alloy, the Ti contribution $m_{\mathrm{Ti}}(k_{\mathrm{Ti}} - 1) = 272$ K is such that even a small amount of Ti can shift the growth domain significantly.

2.2. Mesoscopic and granular modelling approaches

A difficulty of multiscale models is the handling in a single approach of both columnar and equiaxed morphologies [2], although a new approach has been proposed recently [18]. This problem is alleviated in so-called stochastic models of solidification such as the CAFE approach [19], in which the macroscopic continuity equations are solved with a Finite Element method at the scale of the casting, while nucleation and growth models are implemented at a much finer scale of cells. Again, while this CAFE approach has shown its full power for fully dendritic specimens, it is based on the growth kinetics of a dendrite tip and is thus not well adapted to globular–dendritic grains (and large castings).

For fully globular grains, another stochastic approach has been adopted to address the problem of hot tearing formation occurring deep in the mushy zone, i.e. at high solid fraction. First developed in two dimensions [20], this model was extended to three dimensions for small volume elements [21–23]. In this approach, nucleation centres (corresponding for Al-alloys to the positions of the most active TiB_2 particles) are distributed randomly within the volume element. Taking the Voronoï tessellation of these centres, the faces correspond to the final grain boundaries. A solute balance made within each of the Voronoï pyramids allows one to predict the evolution of the solid–liquid interface and the last stage solidification when liquid films are replaced by solid grain boundaries, i.e. coalescence [24]. Feeding through the network of liquid channels and deformation of the already coalesced solid are modelled. This allows us to visualise the percolation of the grains, while a defect criterion can determine at which pressure within the liquid channels cavitation will occur. The hot tear nucleated in this way will then propagate within neighbour liquid channels. This was successfully used to numerically simulate and interpret hot tearing observed under X-Ray tomography, see Fig. 2.

This stochastic hot tearing model corresponds to the so-called RDG (Rappaz–Drezet–Gremaud) criterion [25], which is based on average conservation equations (and thus average strain rate) and is thus similar to Niyama's criterion for the prediction of porosity formation [26]. But it is much more refined in the sense that it can account for the influence on the alloys' hot tearing sensitivity of grain size, grain boundaries and the balance between solid–liquid interfacial energy and grain boundary energy. Coalescence of the primary phase, which dictates the percolation and final solidification stage in dilute alloys, competes with the formation of eutectic in more concentrated alloys: the last eutectic valley where solidification terminates influences shrinkage-driven flow and the associated liquid pressure loss leading to hot tear [27].

2.3. Phase field modelling of Al alloy solidification

Since the first solutal dendrite of Ni–Cu simulated in two dimensions with the phase field method [28], this technique has shown its tremendous power to model microstructure formation in three dimensions (see, for example, [2] or [29]). It is quite intensive in terms of computation power, but this is the method of choice since, first, the shape of the solid–liquid interface is not prescribed (free boundary), and second, a fixed mesh rather than a front-tracking is used. It would be too long to enumerate the many problems addressed with this method, but for aluminium alloys let us mention:

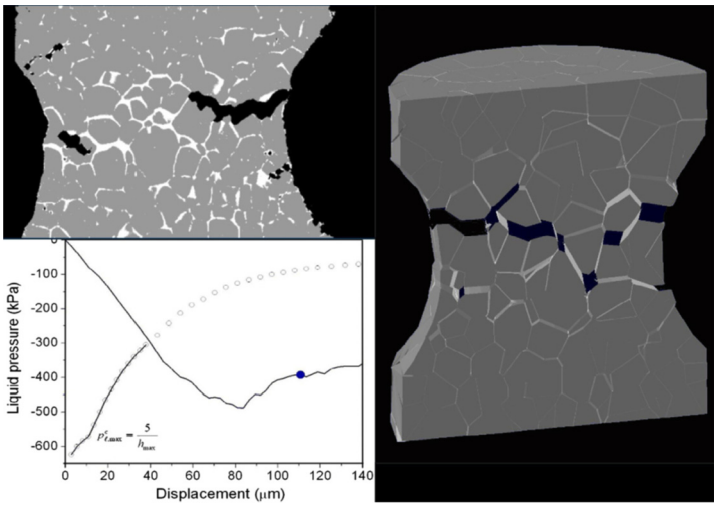

Fig. 2. In situ X-ray tomography observation of hot tear formation at the small notch of a cylindrical Al-8%Cu small specimen under tensile stresses (top left) and comparisons with the prediction of the stochastic hot tearing model (right). The diagram at the bottom left shows the depression in the liquid compared with the cavitation pressure required to nucleate a pore in the widest channel [22].

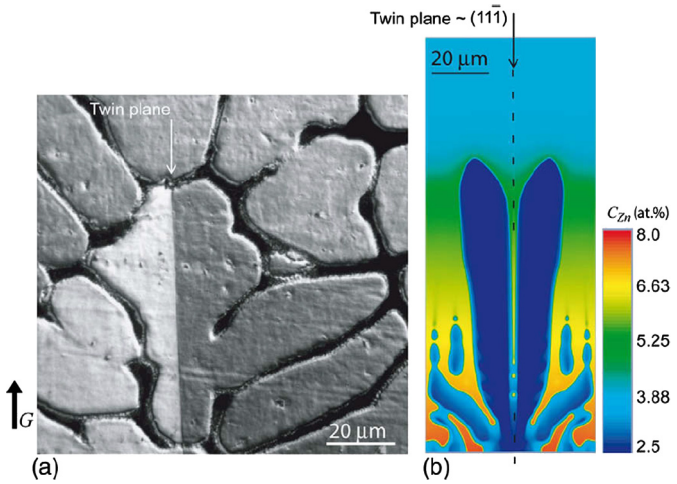

Fig. 3. (a) Longitudinal section of a quenched ⟨110⟩ twinned dendrite in an Al-20 wt% Zn alloy and (b) phase-field calculation of such a morphology with an imposed dihedral angle at the triple line between the twinned solid, un-twinned solid, and liquid in an Al-5 wt% Zn alloy; after M. Salgado's PhD thesis [32].

- the transition from globular to dendritic morphologies [16], which provides conditions relating the cooling rate and the final grain size or grain density [30];
- the growth of twinned dendrites (so-called feathery grains) associated with the formation of a doublon growing along ⟨110⟩ directions [31], see Fig. 3;
- the influence of solute elements such as Zn on dendrite growth directions [33]. With increasing Zn composition, it has been shown that the dendrite growth directions change from ⟨100⟩ to ⟨110⟩ directions, as a result of a change of the solid–liquid interfacial energy anisotropy [34].

2.4. AIMD of alloyed Al melts

An important attribute of aluminium is its ability, with certain alloying elements, to induce local covalent bonding, resulting in strong icosahedral short-range ordering (ISRO) in the liquid. As a consequence, many intermetallic phases reflect this five-fold symmetry of building blocks and many of the quasicrystals (QC), starting with the first one Al_6Mn, are based on aluminium. Ab Initio Molecular Dynamics (AIMD) modelling of liquid alloys gives insight into the atomic interactions governing these cluster arrangements, which in turn govern dynamic properties (diffusion and viscosity) and entropic contribution to crystallisation.

Ab initio modelling computes the behaviour of a restricted number of atoms (typically 500) for a short period of time (typically 500 ps) that is, however, sufficient to capture dynamic properties. Such calculations last typically three months. The relatively small number of atoms does not allow modelling multiconstituent alloys: ternary alloys with not too dilute solutes constitute the horizon of such calculations. In spite of these limitations, AIMD presents a huge potential for guiding alloy design and also for feeding process numerical modelling with thermophysical properties difficult or impossible to measure.

Regarding liquid Al alloys, a*b initio* simulations have been carried out on several systems. Comparison of two compositions either known to form quasi-crystalline phases (Al80Mn20) or known *not* to form QCs (Al80Ni20) shows that in both cases there is a strong chemical order, the solute atoms being surrounded with solvent Al atoms. Whereas Mn atoms are mainly surrounded by Al atoms arranged along an icosahedral symmetry, the short-range order prevailing around Ni atoms is of the *fcc* type [35]. In Al80Mn20 alloy, it was found by AIMD that a key role is played on the SRO by the occurrence of localized magnetic moments of Mn atoms [36]. Other *ab initio* calculations [37] predict that Samarium strongly increases ISRO against *fcc* precursors in liquid Al. Monte Carlo simulations of another Al–RE system, namely Al–terbium, have shown that the special correlation between Tb and Al atoms in the liquid results in nanoscale chemical separation of Tb- and Al-rich regions. A Tb-rich network divides the melt matrix into nanoscopic regions forming isolated clusters of pure Al, in which the initiation of crystallization is inhibited under rapid solidification conditions [38]. In multiconstituent alloys, competition between conflicting ordering patterns becomes very complex and may lead, as described below (§4.1), to demixtion of the liquid into regions exhibiting different dynamics.

Ab initio molecular dynamics simulations were used recently to describe the diffusion of hydrogen in liquid aluminium at different temperatures [39]. Quasi-instantaneous jumps (Levy's flights) separating periods of localized vibrations around a mean position were found to characterize hydrogen motion at the nanoscopic scale. A generalized continuous time random walk (CTRW) model was shown to describe the experimental diffusion coefficients in a satisfactory manner. Such a quantic diffusion mechanism cannot be predicted by empirical potentials, which therefore miss the experimental values by several orders of magnitude.

3. In situ observations of solidification: what they teach about Al solidification

The possibility offered by X-Ray imaging and especially by large instruments such as synchrotrons dedicated to materials science has renewed the interest to visualise solidification mechanisms and phenomena in otherwise opaque metallic melts. Correct representations are essential to innovation and aluminium alloys are ideal for that purpose since they are fairly transparent to X-rays. Studies include X-ray radiography, tomography and topography [40]. We will not mention the usage of such techniques for ex situ 3D-characterisation of specimens already solidified.

Synchrotron monochromatic radiography has been initially used to visualise in situ and in real time dendritic growth in binary aluminium alloys [41,42]. Advances in the technique allowed one to measure local concentrations in the liquid between equiaxed Al grains during the solidification of binary Al–Cu alloys [43]. Recently, an improvement of the synchrotron-based technique for elemental imaging, combining radiography and fluorescence spectroscopy, has been realised and applied to study the spatial distribution of different solutes that can be mapped independently and simultaneously during solidification [44]. This study made heavy use of machine learning to allow for automatic identification of individual growing equiaxed grains. Studies of equiaxed solidification of Al–Cu and Al–Si alloys [45] revealed that the frontier between nucleated regions and non-nucleated regions progresses by successive jumps and that growth rate fluctuates with a periodicity between 0.2 and 0.4 s. This is to be related to the observation of concentration oscillations after the columnar to equiaxed transition in Bridgman solidification of Al–Ni or Al–Si alloys [46]. Synchrotron studies allow for grain counts over time, while *post mortem* analyses only give access to final grain size. Grains appear to rotate to fit into the spaces formed by the previous layer of grains and sometimes vertical channels of liquid between the grains seem to form [45].

Similar relative micro movements between grains and the liquid are also mentioned by a recent study performed in a transparent alloy [47], extending the pioneer work of Hellawell and co-workers [48]. These observations show that the rising of solute-rich less-dense liquid through the dendrite network causes solutal remelting of dendrite arms, entraining them in the bulk of the melt, and thus inducing self-inoculation of the alloy besides macrosegregation. Such self-grain-refining behaviours are experimentally observed in industrial casting of Al–Mg alloys, for example. But these mechanisms may also affect the formation of casting defects such as hot tearing, porosity formation, and eutectic segregated pockets. Movement of the interdendritic liquid can also be induced by mechanical vibration as in the experiments published in [49], which conclude that fluid flow in the permeable dendritic mush may be the key factor for the alteration of the solidification microstructure. Pulsed electromagnetic field may also cause dendrite fragmentation and grain refinement as evidenced in [50]. Thermo-electromagnetic forces can also be created by the interaction between the electric current generated by the thermoelectric effect in the vicinity of the liquid–solid interface submitted to a temperature gradient (Thomson–Seebeck effect) and a static magnetic field. Synchrotron observations evidenced the movement of dendrite fragments during solidification of an AlCu alloy in this configuration [51].

All these observations provide a lot of insight into the various mechanisms, in the absence or in the presence of external fields (besides gravity). The relative movements between the solid and liquid phases induce solutal remelting-activated fragmentation of dendrites and consecutive grain refinement of Al alloys by mechanisms other than allogeneic inoculation. This further suggests process levers for the tuning of industrial solidification structures.

Another stimulating observation is the growth morphology modification of Al dendrites by nanoparticles due to the disturbance of the solute diffusion field caused by interfacially adsorbed nanoparticles, together with a greater degree of freedom left to the dendrite arms for following different directions dictated by the local variation of solute content [52]. In-situ radiography of eutectic formation in Al–Si alloys have allowed one to visualise the effect of Sr on the nucleation and growth of the silicon phase and the early stage of eutectic coupled growth [53]. Combined X-ray radiography and topography under white beam illumination gave some unique information on the deformation of dendrites during directional solidification of alloys [54]. Finally, in situ 3D X-ray tomography (sometimes referred as 4D tomography) is progressing rapidly in time and space resolution. It has been used to visualise coarsening in Al–Cu alloys [55] or even the development of the full network of dendrites in Al alloys [56].

4. Microstructure selection in the solidification of Al alloys

Microstructure selection occurs during all stages of liquid-to-solid transformation. Most of the selection criteria are based on growth kinetics, i.e. *fastest growing phase* (under equiaxed conditions) or *highest growth temperature*. We will see that selection mechanisms controlled by nucleation may fall within either category.

Most of structure selection mechanisms in DC Casting of Al alloys, where isotherm velocity is imposed by the process, are governed by a highest growth temperature criterion. Aluminium alloys illustrate this criterion in specific ways in comparison with other alloy systems, as they exhibit:

- very low anisotropy of the solid–liquid interfacial energy, thus leading to various growth morphologies,
- strong proportion of Icosahedral short-range order (ISRO) of atoms in the liquid, which has many consequences on the nucleation and growth kinetics, the formation of stable or metastable phases e.g., metastable Al–Fe intermetallics, quasicrystals, and the fairly unique tendency to form twinned dendrites [57].

From an industrial point of view, it should also be noted that Al alloy melts can be easily inoculated, through a template effect exerted on the neighbouring liquid by crystalline substrate such as TiB_2 or TiC [58] coupled with a peritectic reaction triggered in 2D at Ti concentrations well below the bulk equilibrium peritectic composition. This template effect locally erases ISRO and orient nucleation from the introduced crystalline precursors.

4.1. Nucleation mechanisms for the primary phase

Besides conventional grain refiners based on titanium borides and carbides, a so far unknown nucleation mechanism has recently been evidenced [59,60] in the {Al–Zn + 1000 ppm Cr} system. EBSD analysis of the as-cast microstructures has revealed a higher than statistically expected density of grain boundaries in a twin relationship. The grains exhibiting such orientation relationships are associated by groups of 5, a signature of the fact that these grains have probably grown from a common, transient quasi-crystalline substrate with 5-fold symmetry. Now, in the Al–Zn + Cr system, a peritectic reaction creates a solid substrate with 5-fold symmetry motifs, namely the complex intermetallic Al_7Cr whose large monoclinic unit cell contains many icosahedral building blocks, with a Cr atom at each centre [61], a direct consequence of the ISRO pre-existing in the liquid. It was thus conjectured that this nucleation mechanism occurs in two steps: first, the formation of small icosahedral quasicrystals in the melt thanks to their low interfacial energy with the liquid, followed by hetero-epitaxy of the *fcc* phase on facets of these quasicrystals, which will thus have mutual twin relationships, see Fig. 4.

This provides ground to the idea that twinned grains growing from the melt – so-called feathery crystals, may nucleate on icosahedral motifs forming from the melt. The recent observation in a non-grain refined AlZnMgCr alloy as cast billet of concomitant feathery crystals and spherical Al cells divided into sectors of different orientations may support this view (Fig. 5).

From the atomistic point of view, the problem of how ISRO can evolve into medium-range order (MRO, that is, beyond the first neighbours) is a central one. AIMD calculations of the Al–Cr and Al–Zn–Cr liquid systems [62] have evidenced a demixtion instability of the liquid by spinodal decomposition into two intertwined families of MRO clusters at no interfacial energy cost (Fig. 6). The Cr-rich MRO regions have significantly slower dynamics than the fast-dynamic regions formed by Al (and Zn) atoms only, this dynamic heterogeneity leading to a breakdown of the Stokes–Einstein relation corresponding to a crossover from the Arrhenius to non-Arrhenius behaviour for diffusion coefficients and viscosity. One scenario is that the slow dynamics regions will serve as sacrificial metastable nucleants for the others as they will disappear by peritectic reaction. In any case, the homogeneous nucleation of iQCs appears as resulting from local fluctuations of icosahedral arrangements of atoms in the liquid until a critical size is reached. It also means that the quasicrystalline order in the liquid is not only at the origin of frustration leading to glass formation, but may also in some cases be regarded as providing the substrate for epitaxial growth of crystalline order [63]. This may have practical implications in the future of Al solidification metallurgy.

This nucleation mechanism belongs to the “fastest growing structure selection criteria” family, as the liquid arrangement evolutions that lead to it correspond to Turnbull’s formula of “what is kinetically preferred within the range of thermodynamic possibilities”. He further commented that “short-range order, whether compositional or topological, can develop *more rapidly* than long*range order” [65]. The recent descriptions published by Tanaka [62,66] fit in this view as the bond

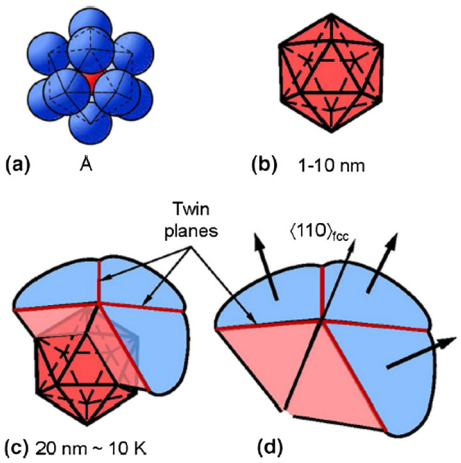

Fig. 4. Schematic diagram showing the iQC mediated nucleation of the fcc phase during solidification: (a) ISRO atomic arrangement in the liquid; (b) formation of iQC; (c) formation of fcc on the iQC with heteroepitaxy relationship; (d) further growth of the fcc with disappearance of iQC during cooling, leaving only multiple twinned fc grains with some common ⟨110⟩ directions; after [59].

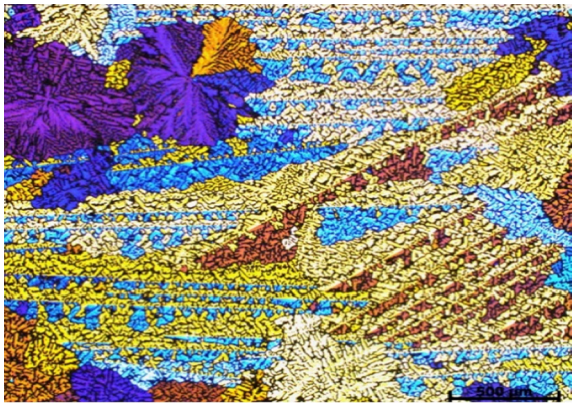

Fig. 5. Concomitant spherical Al cells divided into sectors of different orientations and twinned columnar dendrites in a non-grain refined AlZnMgCr as-cast billet. Both structures may have nucleated on icosahedral motifs formed from the melt (unpublished Constellium results; field width = 2.7 mm).

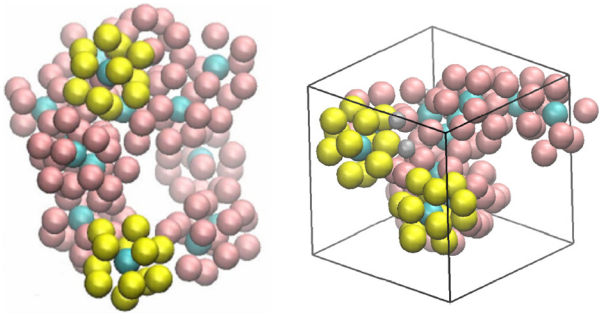

Fig. 6. AIMD calculations of icosahedral medium-range order in undercooled Al–Cr and Al–Zn–Cr melts at 800 K, after [64] and [63]. Cr atoms are drawn in blue, Zn atoms in grey, and Al atoms in pink; Al atoms in two typical Cr-centred icosahedra are highlighted in yellow for visual purpose. Left: Al80Cr20; right: Al83Zn10Cr7, but the local composition in the slow dynamics region is found to be Al85Zn3Cr12.

orientational order (BOO) initially increases without any change in the packing density (inhomogeneous supercooled liquid with crystal-like BOO fluctuations), followed by continuous increase in the phase coherency of crystal-like BOO in a region of high density and eventually the formation of a crystalline phase due to the development of a translational order induced by the growth of crystal-like BOO.

The above-mentioned ab initio molecular dynamics studies suggest that the introduction of slow-diffusing solutes in Al alloys will promote the formation of dynamic heterogeneities in the undercooled melt, which may either trigger some kind of homogeneous nucleation in the case of peritectic solutes (because the slow-dynamics, solute-rich zones have a higher

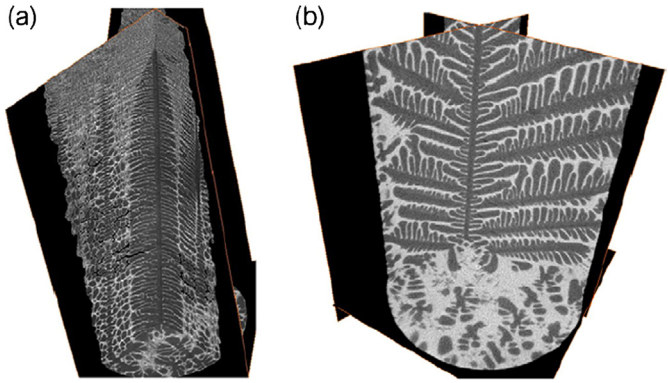

Fig. 7. Transverse and longitudinal sections of a 3D X-ray tomography reconstruction of quenched Al–Zn dendrites solidified in a Bridgman furnace at 4 mm/min, showing the growth of (a) ⟨100⟩ dendrites in Al-10 wt% Zn and (b) ⟨110⟩ dendrites in Al-90 wt% Zn. From [68].

freezing point), or affect intermetallic selection or primary Al growth morphology in relation with slower diffusion kinetics of the partitioning solutes. In particular, at the onset of primary Al solidification the selected growth pattern will be more dendritic because more exchange area is needed for the partitioning of slow diffusing solutes.

Under this perspective, the fact that many quasicrystalline systems were found in Al-based alloys and the large number of complex intermetallics being crystalline approximants of icosahedral phases is a consequence of the versatility of Al melts atomic arrangements and of the propensity for dynamic heterogeneities that recent AIMD calculations have revealed; of particular interest in the selection of the fastest growing arrangements is the behaviour of those clusters, which cannot unambiguously be attributed to icosahedral SRO or cubic SRO and strongly depends upon composition: what makes them evolve into either of the two dominant short-range order types in the cooling melt is an open question.

Likewise, introducing substrates for heterogeneous nucleation can be seen as a way of guiding or forcing the configurational path, through a template effect exerted on the neighbouring liquid. But the physical mechanisms of nucleation are fundamentally the same: be it through the introduction of solute elements that modify the path toward medium-range order, or through the introduction of crystalline substrates that do so by imprinting crystalline order to the neighbouring liquid layers, the problem can be summarized as being the study of the lesser entropy path in the configurational space.

4.2. Primary phase morphology

Under directional solidification conditions (constrained growth), pattern selection in dendritic growth falls within the category of the higher temperature – or minimal undercooling – selection criteria, if we consider a given phase. Neglecting the contribution from the attachment kinetics of atoms (or clusters of atoms), it is linked to the crystal-melt interfacial free energy $\gamma_{s\ell}$. A general discussion of the atomistic ground for interfacial thermo-kinetics of metallic crystals can be found in [67]. Without anisotropy of $\gamma_{s\ell}$, it has been shown that seaweed-like grains form rather than dendrites. In simple cases, an anisotropy of $\gamma_{s\ell}$ leads to dendrites growing along maxima of the interfacial energy, or more precisely minima of the interface stiffness defined as $\gamma_{s\ell}$ + the second derivative of $\gamma_{s\ell}$ along the principal radii of curvature. For a cubic crystalline phase such as Al, two anisotropy parameters, ε_1 and ε_2, characterize the first- and second-order terms in a cubic harmonic expansion of $\gamma_{s\ell}(\mathbf{n})$, where $\mathbf{n}$ is the unit normal in three dimensions. Aluminium is known to have a weak anisotropy of $\gamma_{s\ell}(\mathbf{n})$, typically $\Delta\gamma_{s\ell}/\gamma_{s\ell}$ is of the order of 1%, i.e. the two terms ε_1 and ε_2 are weak and can be influenced by solute elements. Although a competition between ⟨100⟩ and ⟨110⟩ dendrite growth appears to be an intrinsic feature of *fcc* crystals that exhibit positive ε_1 and negative or zero ε_2; it is best exemplified for Al alloys. Such a dendrite orientation transition (DOT) has been observed in Al–Zn, as the zinc composition is increased from 20wt% to 60wt% [68]; see Fig. 7.

Instead of the standard ⟨100⟩ growth direction, the directions ⟨110⟩ and ⟨211⟩ have been observed in Al–Cu–Mg alloys when the temperature gradient and the growth speed were varied [69] – see Fig. 8 – or even ⟨320⟩ [71]. Selection of the ⟨111⟩ growth direction was also recently observed in rapidly solidified Al–Cu droplets [70]. It is to be noted that, as the speed is increased, the criterion based on the anisotropy of $\gamma_{s\ell}(\mathbf{n})$ might be influenced, or overruled, by the anisotropy associated with the attachment kinetics anisotropy of ISRO building blocks.

Similarly, growth morphologies of equiaxed grains or of the eutectic aggregate are some of the features that are selected along a fastest growth criterion. This is of metallurgical interest, and relationships between the grain refinement strategy and microstructure selection have long been noted [72,73], leading to metallurgy-driven optimisation of solidification parameters. It has also been noted that the morphology and the extent of interconnectivity of intermetallics rather than their specific type may make the as-cast structure problematic for further downstream processing [74]. Such topological patterns of intermetallic size and distribution were explicitly related to the grain refinement strategy [75,76] as dendritic morphologies were found to promote finer and more homogeneous distribution of constituent particles, which poses the problem of dendrite morphology selection through the grain refinement strategy.

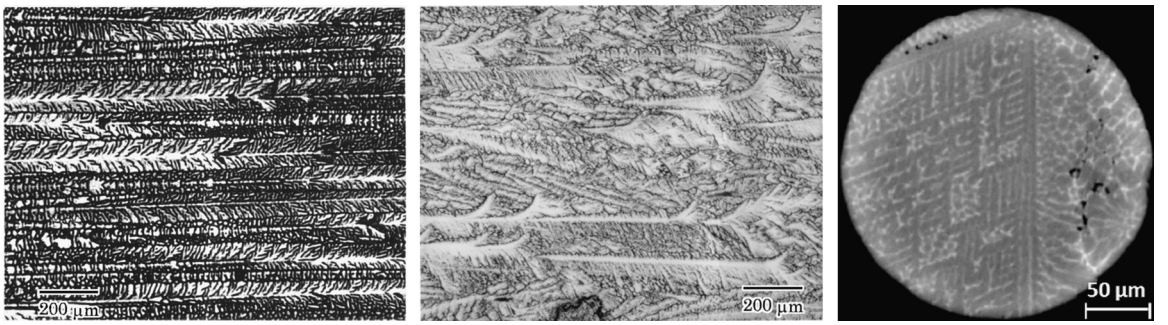

Fig. 8. Left: Al-4.3%Cu-0.3%Mg alloy 1D-solidified under a gradient of 130 °C/cm at 1 mm/s), growth directions ⟨110⟩ and ⟨211⟩; centre: growth direction change during a solidification experiment, same alloy, curved dendrites obtain at 1 mm/s under a gradient of 230 °C/cm;) source: S. Henry's PhD thesis [69] On the right, synchrotron X-ray micro-tomography cross section in an Al-4.5 wt% Cu rapidly solidified droplet showing a ⟨111⟩ dendritic structure [70].

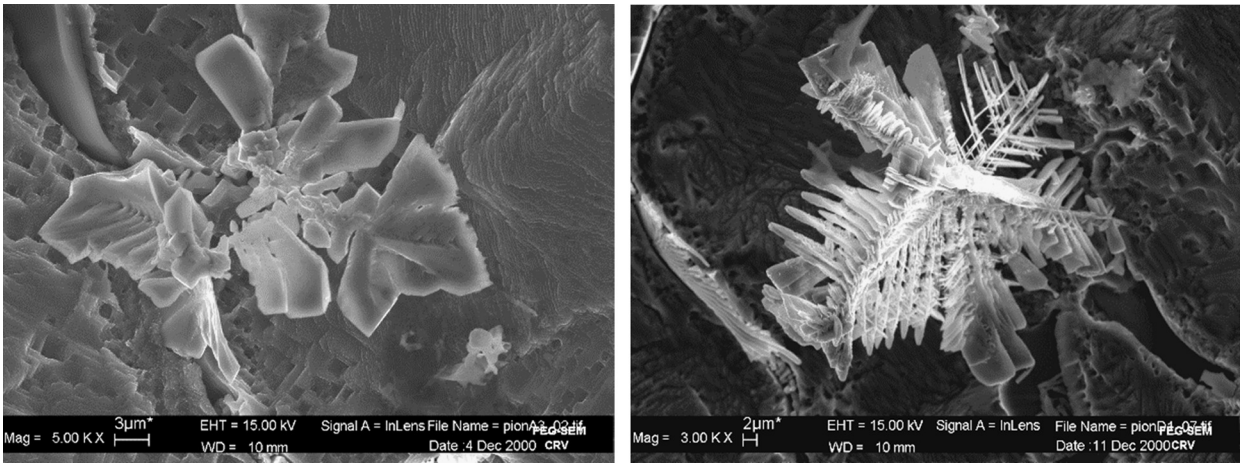

Fig. 9. Aspect of AlCuFe(Si) intermetallic particles after partial dissolution of Al matrix in an as-cast AlZnMgCu alloy; left: no modification; right: modification by barium. (Source: Constellium.)

4.3. Nucleation and growth of intermetallics

In the Al–Si eutectic growth, the adsorption of large, tensioactive alkaline or alkaline earth or rare-earth atoms on Si facets has been understood since the 1980s [77] to provide further branching ability to the anisotropic faceted Si phase via an impurity-induced twinning (IIT) mechanism, making coupled growth possible. Recent experiments coupled with DFT calculations have confirmed the validity of this mechanism [78]. A probably similar twinning mechanism has been obtained with barium additions to modify Al_7Cu_2Fe growth in AlZnCuMg [79] (see Fig. 9).

Recent advances in the understanding of the Al–Si eutectic modification are related to a better knowledge of Al–Si–P ternary diagrams [80] and of phosphorus scavenging elements (AlP being a nucleant for primary Si as the lattice parameters of AlP cubic zinc blende, and Si cubic diamond, are respectively 5.421 Å and 5.430 Å). The formation enthalpy of Sr_3P_2 being more negative than that of AlP, strontium not only modifies the growth of Si by IIT, but also partially inhibits the AlP nuclei present in the melt. The same is reported for Ca, forming the Ca_3P_2 compound. Also, in AlSi alloys with additions of Ca, Sr, Y or Yb, the Al_2Si_2Ca [81], Al_2Si_2Sr [82], Al_2SiY [83], Al_2Si_2Yb [84] phases were reported to deactivate the nucleation potency of the AlP phase for primary Si, either by taking some P in solution, or by nucleating on AlP particles prior to primary Si, while being themselves poor nucleants for primary Si.

Some studies suggest that the addition of Sr also alters the liquid structure around the growing Si. Diffraction data for liquid alloys Al-3%Si, Al-7%Si, Al-10%Si, Al-12.5%Si (all wt%) were obtained at various melt temperatures (5–220 K) above the respective liquidus temperatures [85]. It was observed that the addition of 0.04 wt% Sr results in significant change in the liquid structure parameters, such as structure factor, pair distribution function, radial distribution function, coordination number and packing density. It is probable that the Si growth modification is due to other dominant factors (see above); however, the role of Sr on the Al melt structure is enlightening for other reasons: it is expected more generally that solutes altering the diffusion kinetics of species near the interface of a growing intermetallic will play a role on intermetallic selection. This is to be linked to the known and opposite influences of transition metals or large alkaline earths on Al–Fe stable *vs* metastable intermetallics selection in Al alloys, while Cr [86], V [87], or Cu [88] are known to promote selection of metastable Al_mFe phases at lower isotherm velocities; Ca, on the contrary, is known to expand the stability domain of

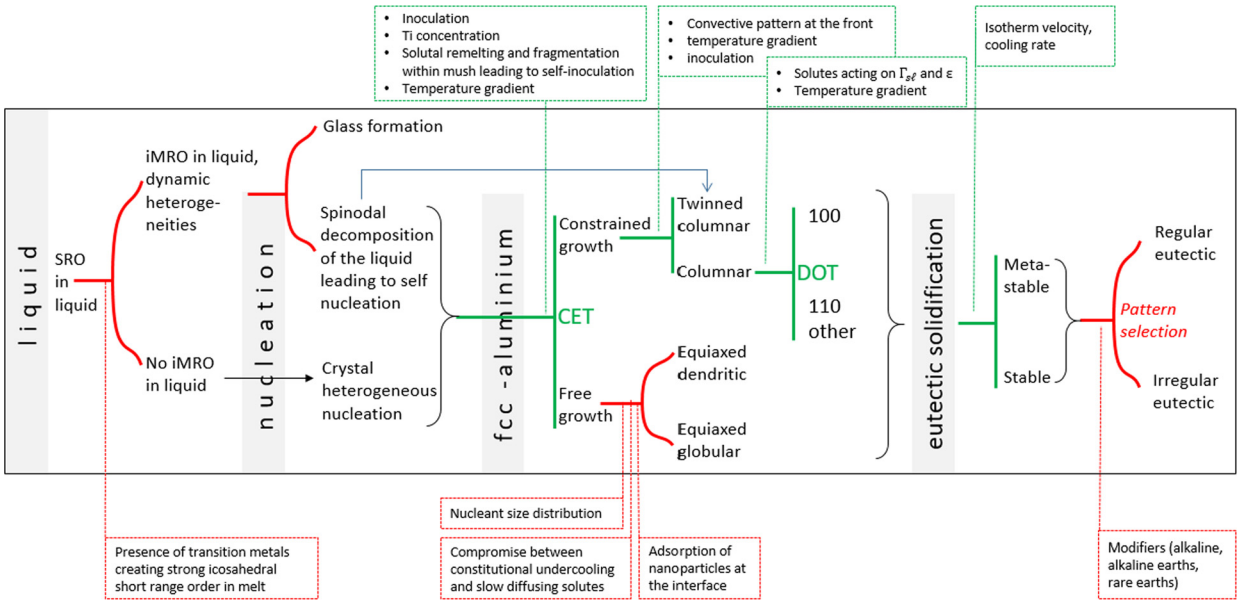

Fig. 10. Synthetic chart of possible selection steps from the liquid to the last forming solid in Al alloys solidification. Red curved forks: selection along a fastest growth criterion; green straight Ts: selection along a highest growth temperature criterion. CET = columnar equiaxed transition; DOT = dendrite orientation transition. Labels above, resp. below the chart list the main metallurgical levers relevant to the selection mechanisms, minimum undercooling, resp. fastest growth selection criterion.

the equilibrium $Al_{13}Fe_4$ phase to higher isotherm velocities [89,90]. Now Cr or V slow down atomic dynamics by increasing ISRO in the melt, while Ca, like Sr, is expected to decrease ordering of the melt, thus to increase atom mobility. It thus appears that metastable *vs* stable Al–Fe phase selection is governed by diffusion restrictors *vs* diffusion enhancers in the liquid. Prediction of these transport properties by *ab initio* modelling of the liquid is thus a potentially efficient tool for alloy designing.

4.4. Synthesis of selection mechanisms in Al alloys solidification

We propose here a synthetic view of the possible selection mechanisms from the liquid state to eutectic solidification at the end of the solidification path of an Al alloy (Fig. 10). The curved red forks represent the selection of the fastest growing structure, while the green, straight T-lines represent the selection of the structure growing at the minimum undercooling.

In the liquid state, medium-range order, that is proto-nucleation when it develops around peritectic elements, may develop faster than long range order, leading to the selection of either a homogeneous nucleation mode [59], or glass formation if iMRO takes over, depending on the cooling rate and the composition.

In general, except when micro-convection movements in the mush allow solutal remelting and dendrite fragments release, heterogeneous nucleation is necessary for an equiaxed growth of Al alloys, and a lower undercooling selection criterion will apply for the activation of the larger nuclei. However, equiaxed growth will overcome columnar (constrained) growth only if columnar undercooling is sufficiently large (and the temperature gradient sufficiently low). It is well known that for a given alloy, Ti concentration plays a major role, as small Ti amounts provide a lot of constitutional undercooling [$m(k-1) = 272$ K], thus depressing the columnar growth temperature.

Then, while columnar *vs* equiaxed selection, or the selection of the nuclei for equiaxed growth, belong to a smaller undercooling criterion, the growth morphology of equiaxed grains is selected along a fastest growth criterion. The local solute diffusion field governs dendrite growth and parameter variations such as an increase in nucleation undercoolings (with smaller nuclei) or the presence of slow-diffusing solutes will cause a larger interfacial area to develop for diffusion to occur in the available time. This may select faster dendritic growth over sluggish globular growth.

In the case of constrained growth, Al alloys have the peculiarity of developing twinned columnar grains that probably result from the growth of doublons (see above). The groove at the middle of the tip accumulates solute, which allows for a reduction of the solute rejection ahead of the tip and of the corresponding constitutional undercooling, hence the growth advantage [57].

5. Alloy design for additive manufacturing

The ever-growing interest for the possibilities offered by Additive Manufacturing (AM) stimulates revisiting rapid solidification studies that date back to the 1980s and 1990s in a renewed process context. Use of interface response function

theory to describe non-equilibrium solidification during welding and AM is being used by several teams. Usually, the approach consists in using a solute-trapping model like the classical one by Aziz [91] or a more-refined one such as developed by Galenko [92] and a velocity-dependent liquidus slope (asymptotically tending toward the T_0-line). Such a model can be coupled with the equations governing the dendrite tip radius and the solid–liquid interface compositions [93]. Knowledge acquired in welding studies is valid, but boundary conditions have to be revisited for the specific case of AM.

Rapid solidification not only involves solute trapping, but also precipitation of metastable phases:

- in the Al–Zr system, cubic $L1_2$ Al_3Zr, which exhibits a lattice parameter very close to that of Al, is selected at high cooling rates instead of the equilibrium tetragonal varieties [94,95], therefore acting as nuclei for fine equiaxed grains at the bottom of the pool during lasing;
- the formation of metastable quasicrystals has also been explored to reinforce Al alloys processed by rapid solidification: according to Tsai [96], the icosahedral order is in equilibrium in the liquid state above the liquidus for stable iQCs, whereas the icosahedral order prevails in the undercooled liquid state for metastable iQCs. In this respect also, AIMD calculations of undercooled compositions may prove useful for alloy design.

As some amount of solute trapping is usually sought for to increase hardness or the ability to precipitate hardening (meta)stable phases from the supersaturated solid solution in order to improve medium high temperature properties, alloys are developed, which exhibit low atomic mobility in the liquid state. However, slower diffusion goes along with larger viscosity through the Stokes–Einstein law, which states that the product of diffusivity by viscosity is equal to $k_B T/2\pi R$, where T is the temperature and R is the position of the first peak of the pair correlation function. Too high viscosity as in amorphisable melts may thus hinder processability. AIMD calculations of the liquid alloys structure give access to the prediction of diffusion coefficients and viscosities in relation with the amount of cage effect caused by ISRO (see for example [97] for aluminium alloys). They can predict under which conditions the Stokes–Einstein law breaks down along with the appearance of dynamic heterogeneities at medium range. They also give access to solid–liquid interfacial tensions [98].

But alloy design for selective laser melting (SLM) must also account for processability. Although the laser beam speed might be high, that is, melting is rapid, solidification is still controlled by the thermal gradient behind the molten pool. The latter depends on many factors: overall shape of the object, trajectory of the laser beam source, and heat transfer among various media (laser beam, consolidated *vs* unprocessed powder, ambient air...). For smaller objects, the laser is positioned in a restricted area, and the overall component heats up, thus reducing the thermal gradient (and solidification speed), making the process closer to the Osprey process. For large dimensions, solidification might become indeed rapid and equilibrium might be lost at the solid–liquid interface. The powder bed that has not yet been processed acts somehow as a thermal insulator, and conduction occurs mainly through the already consolidated solid. Interaction of the laser with the powder bed involves complex mechanisms of reflection and absorption; liquid droplets coalescence depends upon their surface tension and the oxide layer present at the surface of the powder grains; strong powder ejection, droplets trying to grow but not succeeding because of the laser itself, and porosity formation by gas trapping due to the dynamics of the melt pool, all contribute to processability. In SLM, if the energy input is sufficiently high, the peak temperature in the melt pool can reach the boiling point and vaporisation of metal from the melt can occur: this regime is referred to as *keyhole* melting mode. The complex physics of keyhole melting, including vaporisation and recoil pressure exerted by the vapour on the melt pool, have been studied recently [99]. Increase of laser power causes deeper penetration, improved remelting of powder grains and increased productivity, but this is at the detriment of metal quality as there is gas entrapment by keyhole depression collapse. On the other hand, increasing scanning speed for productivity reasons causes the so-called balling effect, that is, the molten track coalesces in separated drops according to a Rayleigh–Plateau instability mechanism, with non-melted zones in between [100]. A capillary stability analysis of the melt pool has been proposed, rationalising its dependency upon scanning velocity, powder layer thickness, and the material optical and thermal properties [101]. Various high-speed imaging techniques of melt track progression and powder movement under the influence of laser melting and vaporising [102–104] emphasize the overwhelming influence of coupling between heat flow, fluid flow (both gas and melt), including Marangoni convection and hydrodynamic instabilities. They provide essential insight to the physical parameters that have to be accounted for in alloy design for processability. In turn, alloy acceptability for SLM processing may be enhanced by progresses in melt pool instability control: for example, it has been shown that the grain morphology can be tailored by varying beam intensity spatial profile while maintaining constant laser power and scan speed [105]; likewise, beam oscillation in laser welding at typical frequencies of 500 Hz and sub mm amplitudes has been shown to allow for melt pool depth tuning and reduction of hot cracking [106]: such welding process advances are being transferred to the field of SLM.

6. Coupling of scales: role of fluid flow in solidification

Fluid flow interacts with solidification at both the microscopic scale (interaction with the solutal diffusion fields, influencing growth direction and morphology) and macroscopic scale (transport and separation of solid and liquid phases with different compositions leading to macrosegregation).

Fluid flow is present everywhere in casting processes. Liquids are self-adapting bodies that organize themselves under body force fields, forming steady recirculation structures whose time constants are often commensurable with solidifica-

tion typical times; hence their decoration with compositional and structural heterogeneities. This explains why stirring the melt during solidification usually creates macrosegregation; let us mention for example the reported formation of fishbone-like macrosegregation during upward solidification of a small Al–Si cylindrical ingot when a rotating magnetic field is imposed [107,108]. Reciprocally, it is to be expected that fluid flow control by means of external fields might prevent recirculation patterns from spontaneously establishing and forming macrosegregation patterns. Fluid flow instability control has recently made dramatic progress: for example, vortex shedding in the wake of a cylinder could be successfully suppressed for the first time in 2015 [109] thanks to a non-linear stability approach; likewise, flame control was achieved [110]. This was made possible by the fact that stability theory is now not only able to predict the growth of unstable patterns but also to specify those areas of the flow where the growth of instabilities is most likely to be impeded by external forcing (so-called sensitivity and receptivity analysis). Additionally, stability theory can now be applied to unsteady states by means of Floquet theory. It is therefore to be expected that application of this knowledge might provide scope for important progress in many casting processes where flow instability is associated with defect formation as, for aluminium, continuous casting melt inlet, vertical semi-continuous casting sump, welding or additive manufacturing pool, etc. Various flow actuators have been explored. Influence of forced flow direction [111] or of inlet flow [112] upon macrosegregation and microstructure has been studied, showing significant influence on the macrosegregation pattern and amplitude; this leads to tuning the flow pattern and grain transport by controlled flow velocity from the spout [113,114]. Besides this direct use of the liquid metal inlet, acoustic streaming (generated by sonotrodes) or traveling or rotating magnetic fields have been used to tune the solidification structure and segregation [115].

7. Conclusion and perspectives

Recent advances in the metallurgy of Al alloy solidification concern all scales: from that of atom cluster arrangements in the melt leading to a renewed understanding of nucleation and phase selection, to the variability of dendritic growth morphology anisotropy, up to fluid flow at the scale of the melt pool of the concerned casting processes and the corresponding macrosegregation phenomena. These advances point out that it is necessary to account for the strong and complex coupling between physical phenomena at different scales to correctly describe solidification structure formation. Use of large instruments together with fantastic progresses in numerical modelling are the most prominent tools fostering these advances, but more traditional, quantitative and semi-quantitative, metallography, such as EBSD, have allowed one to make essential steps forward.

AIMD modelling of liquid Al alloys recently renewed our understanding of nucleation and phase selection. Transition from SRO to MRO in Al-TM liquid alloys is now understood to be accompanied by the demixtion of the liquid into two intricate liquid phases with heterogeneous dynamics. Whereas icosahedral short-range ordering of the melt was thought to be a path to amorphisation through long-range ordering inhibition, it has been recently understood that the TM-rich regions of the de-mixed undercooled melt with slower dynamics could also either serve as templates for the nucleation of *fcc*-Al as in the recently explored Al–Zn + Cr system or prefigure (metastable) intermetallic selection.

At larger scales, there is such a strong influence of the solidification process on the solidification structure, and such a strong coupling between scales through fluid flow, that casting process studies and solidification studies have to be carried out jointly. The development of numerical modelling has thus combined process- and solidification structure-modelling, whereas scale bridging has been a constant necessity and the object of many numerical developments. Modelling therefore not only provides better representation and insight into the phenomena involved in solidification and casting of aluminium alloys, it also suggests engineering ways of acting directly where it is most efficient. To cite two examples: the recent model-based understanding of how the “grain factory” operates in DC casting suggests to act on melt flow to tune grain nucleation and growth and eventually act on macrosegregation and grain morphology [10], and the understanding of the localisation of the last liquid grain boundaries involved in hot cracking, governed by percolation of grain coalescence, where grain growth, grain disorientations, grain size, presence of tensioactive atoms and fluid flow in the remaining intergranular interstices all play a role [20,23].

This is also why synchrotron studies of solidification have proven so useful. The metallurgy of Al has luckily benefited from the possibility to combine a light matrix with heavy solutes, thus providing excellent contrast at not too high melting temperatures; quantified visualisation of nucleation and growth in Al-based alloys have led, among other interesting observations, to reconsider our averaged, simplistic view of nucleation, recalescence and growth by evidencing the major role of solute fields and transport at the microscale. Radiographic studies have also proven to be a precious way of understanding the complexity of processes such as grain refinement, welding or selective laser melting of powder beds, pointing out processability concerns in relation with complex, diphasic flows and surface effects.

In view of the recent progress and developments in the field of solidification of Al alloys, it is thus possible to map out some tentative perspectives for a roadmap to Al alloys solidification science:

(1) fully account for the influence of liquid structure in solidification science: systematic investigation of short-range order, of the path to medium-range order in liquid (undercooled) melts, the understanding of the role played by atom pairs which cannot be unambiguously assigned to a precise motif and may govern the path to crystallisation or amorphisation, are all promising research avenues. The use of AIMD should only grow in the field of alloy design for rapid

solidification as by construction this kind of simulation, for computing time reasons, really describes rapid quenching of melts;

(2) draw maximum information from experimental and synthetic visualisation techniques: machine learning and big data approach make it possible to derive physically-based behaviour laws from loads of both experimental (as in the recent examples of in situ X-ray studies of nucleation phenomena [44]) and synthetic data such as phase-field modelling results (as in the recent derivation of scaling laws for equiaxed growth of Al–Cu alloys [116]);

(3) use of external fields should continue to evolve from the lab curiosity stage to industrial processes, especially for the tuning of fluid flow aiming at optimising the resulting solidification structures, which leads to the following point;

(4) fertilise solidification and especially casting technologies by the most advanced fluid mechanics: tight collaboration between the solidification community and the theoretical fluid mechanics community is needed to fully understand and control the coupling between solidification and hydrodynamic instabilities which is omnipresent in solidification in a wide gamut of scales;

(5) finally, from the engineering point of view, a change in mind-set has started to occur and will only expand, which consists in accounting for the detail of casting heredity in subsequent downstream solid-state transformations of aluminium alloys, as solid-state diffusion scales are set at the solidification stage in tight relation with grain refining strategies and micro-alloying, together with the spatial distribution of constituent particles (mostly Fe-bearing intermetallics) that play such a determinant role in recrystallization, nucleation, damage initiation, and formability of Al-based metallurgical products.

Acknowledgements

PJ gratefully thanks Constellium Technology Centre for having allowed him to publish the present synthesis.

References

[1] P. Jarry, Langages de l'ingénieur, langages de la science, présenté à Langages scientifiques, Grenoble, Maison des sciences humaines, Université Stendhal, Grenoble, France, 1998.
[2] A. Karma, D. Tourret, Atomistic to continuum modeling of solidification microstructures, Curr. Opin. Solid State Mater. Sci. 20 (2016) 25–36.
[3] M. Rappaz, Modeling and characterization of grain structures and defects in solidification, Curr. Opin. Solid State Mater. Sci. 20 (2016) 37–45.
[4] M. Založnik, A. Kumar, H. Combeau, M. Bedel, P. Jarry, E. Waz, The coupling of macrosegregation with grain nucleation, growth and motion in DC cast aluminum alloy ingots, in: J.F. Grandfield, D.G. Eskin (Eds.), Essential Readings in Light Metals, Springer International Publishing, Cham, Switzerland, 2016, pp. 848–853.
[5] M. Bedel, K.O. Tveito, M. Založnik, H. Combeau, M. M'Hamdi, A model study of the impact of the transport of inoculant particles on microstructure formation during solidification, Comput. Mater. Sci. 102 (2015) 95–109.
[6] M. Rappaz, P. Thévoz, Solute diffusion model for equiaxed dendritic growth — analytical solution, Acta Metall. 35 (1987) 2929–2933.
[7] J. Ni, C. Beckermann, A volume-averaged two-phase model for transport phenomena during solidification, Metall. Mater. Trans. B 22 (1991) 349–361.
[8] C.Y. Wang, C. Beckermann, Equiaxed dendritic solidification with convection: Part I. Multiscale/multiphase modeling, Metall. Mater. Trans. A 27 (1996) 2754.
[9] Y. Souhar, V.F. De Felice, C. Beckermann, H. Combeau, M. Založnik, Three-dimensional mesoscopic modeling of equiaxed dendritic solidification of a binary alloy, Comput. Mater. Sci. 112 (2016) 304–317.
[10] M. Bedel, M. Založnik, A. Kumar, H. Combeau, P. Jarry, E. Waz, Influence of transport mechanisms on nucleation and grain structure formation in DC cast aluminium alloy ingots, IOP Conf. Ser., Mater. Sci. Eng. 27 (2012) 012070.
[11] L. Heyvaert, M. Bedel, M. Založnik, H. Combeau, Modeling of the coupling of microstructure and macrosegregation in a direct chill cast Al–Cu billet, Metall. Mater. Trans. A 48 (2017) 4713–4734.
[12] M.C. Flemings, R. Mehrabian, G.E. Nereo, Macrosegregation: Part II, Trans. Metall. Soc. AIME 242 (1968) 41.
[13] T. Jalanti, Étude et modélisation de la macroségrégation dans la coulée semi-continue des alliages d'aluminium, EPFL, Lausanne, Switzerland, 2000.
[14] C. Beckermann, J. Ni, Simulations of sedimentation in globulitic alloy solidification, Int. Commun. Heat Mass Transf. 23 (1996) 315–324.
[15] A. Olmedilla, M. Založnik, H. Combeau, DEM simulation of dendritic grain random packing: application to metal alloy solidification, EPJ Web Conf. 140 (2017) 06002.
[16] H.-J. Diepers, A. Karma, Globular–dendritic transition in equiaxed alloy solidification, in: Solidification Processes and Microstructures – A Symposium in Honor of Wilfried Kurz, 2004, p. 369.
[17] P. Jarry, Recovery vs structure driven DC casting process optimisation, in: Proc. Light Met. Conf. TMS, 2009.
[18] N. Leriche, H. Combeau, C.-A. Gandin, M. Založnik, Modelling of columnar-to-equiaxed and equiaxed-to-columnar transitions in ingots using a multi-phase model, IOP Conf. Ser., Mater. Sci. Eng. 84 (2015) 012087.
[19] C.-A. Gandin, J.-L. Desbiolles, M. Rappaz, P. Thévoz, A three-dimensional cellular automaton–finite element model for the prediction of solidification grain structures, Metall. Mater. Trans. A 30 (1999) 3153.
[20] S. Vernède, J.A. Dantzig, M. Rappaz, A mesoscale granular model for the mechanical behavior of alloys during solidification, Acta Mater. 57 (2009) 1554–1569.
[21] M. Sistaninia, A.B. Phillion, J.-M. Drezet, M. Rappaz, A 3-D coupled hydromechanical granular model for simulating the constitutive behavior of metallic alloys during solidification, Acta Mater. 60 (2012) 6793–6803.
[22] M. Sistaninia, S. Terzi, A. Phillion, J.-M. Drezet, M. Rappaz, 3-D granular modeling and in situ X-ray tomographic imaging: a comparative study of hot tearing formation and semi-solid deformation in Al–Cu alloys, Acta Mater. 61 (2013) 3831–3841.
[23] M. Sistaninia, J.-M. Drezet, A.B. Phillion, M. Rappaz, Prediction of hot tear formation in vertical DC casting of aluminum billets using a granular approach, JOM 65 (2013) 1131–1137.
[24] M. Rappaz, A. Jacot, W. Boettinger, Last-stage solidification of alloys: theoretical model of dendrite-arm and grain coalescence, Metall. Mater. Trans. A 34 (1999) 449.
[25] M. Rappaz, J.-M. Drezet, M. Gremaud, A new hot tearing criterion, Metall. Mater. Trans. A 30 (1999) 449.
[26] E. Niyama, T. Uchida, M. Morikawa, S. Saito, AFS Int. Cast Met. J. 6 (2) (1981) 16–22.

[27] P. Jarry, Hot tear criterion accounting for last stage precipitation in the solidification path: walking in Michel Rappaz' footsteps, in: Symposium in Honor of Michel Rappaz, Nashville, 2016, p. 243.
[28] J.A. Warren, W.J. Boettinger, Numerical simulation of dendrite alloy solidification using a phase field method, in: SP97, 1997, p. 422.
[29] I. Steinbach, Why solidification? Why phase field?, JOM 65 (2013) 1096–1102.
[30] J.A. Dantzig, M. Rappaz, Solidification, EPFL-Press, Lausanne, Switzerland, 2008.
[31] M.A. Salgado-Ordorica, J.-L. Desbiolles, M. Rappaz, Study of the twinned dendrite tip shape I: phase-field modeling, Acta Mater. 59 (2011) 5074–5084.
[32] M. Salgado, Characterization and Modelling of Twinned Dendrite Growth, EPFL, Lausanne, Switzerland, 2009.
[33] J.A. Dantzig, P. Di Napoli, J. Friedli, M. Rappaz, Dendritic growth morphologies in Al–Zn alloys—Part II: phase-field computations, Metall. Mater. Trans. A 44 (2013) 5532–5543.
[34] T. Haxhimali, A. Karma, F. Gonzales, M. Rappaz, Orientation selection in dendritic evolution, Nat. Mater. 5 (2006) 660–664.
[35] N. Jakse, O. Lebacq, A. Pasturel, Ab initio molecular-dynamics simulations of short-range order in liquid Al80Mn20 and Al80Ni20 alloys, Phys. Rev. Lett. 93 (2004).
[36] N. Jakse, A. Pasturel, Local order of liquid and undercooled transition metal based systems: ab initio molecular dynamics study, Mod. Phys. Lett. B 20 (2006) 655–674.
[37] X.W. Fang, C.Z. Wang, Y.X. Yao, Z.J. Ding, K.M. Ho, Competition between fcc and icosahedral short-range orders in pure and samarium-doped liquid aluminum from first principles, Phys. Rev. B 83 (2011).
[38] M. Ovun, M.J. Kramer, Y.E. Kalay, Structural modeling of liquid and amorphous Al91Tb9 by Monte Carlo simulations, J. Non-Cryst. Solids 405 (2014) 27–32.
[39] N. Jakse, A. Pasturel, Hydrogen diffusion in liquid aluminum from ab initio molecular dynamics, Phys. Rev. B 89 (17) (2014).
[40] H. Nguyen-Thi, et al., On the interest of synchrotron X-ray imaging for the study of solidification in metallic alloys, C. R. Phys. 13 (2012) 237–245.
[41] R.H. Mathiesen, L. Arnberg, K. Ramsøskar, T. Weitkamp, C. Rau, A. Snigirev, Time-resolved X-ray imaging of aluminum alloy solidification processes, Metall. Mater. Trans. B 33 (2002) 613.
[42] H. Nguyen Thi, et al., Preliminary in situ and real-time study of directional solidification of metallic alloys by X-ray imaging techniques, J. Phys. D, Appl. Phys. 36 (2003) A83.
[43] A. Bogno, H. Nguyen-Thi, G. Reinhart, B. Billia, J. Baruchel, Growth and interaction of dendritic equiaxed grains: in situ characterization by synchrotron X-ray radiography, Acta Mater. 61 (2013) 1303–1315.
[44] E. Liotti, et al., Mapping of multi-elements during melting and solidification using synchrotron X-rays and pixel-based spectroscopy, Sci. Rep. 5 (2015).
[45] A. Prasad, et al., Real-time synchrotron x-ray observations of equiaxed solidification of aluminium alloys and implications for modelling, IOP Conf. Ser., Mater. Sci. Eng. 84 (2015).
[46] H. Jung, N. Mangelinck-Noël, H. Nguyen-Thi, B. Billia, Columnar to equiaxed transition during directional solidification in refined Al-based alloys, J. Alloys Compd. 484 (2009) 739–746.
[47] M. Stefan-Kharicha, A. Kharicha, M. Wu, A. Ludwig, On the coupling mechanism of equiaxed crystal generation with the liquid flow driven by natural convection during solidification, Metall. Mater. Trans. A 49 (5) (2018) 1708–1724.
[48] G. Hansen, A. Hellawell, S. Lu, R. Steube, Some consequences of thermosolutal convection: the grain structure of castings, Metall. Mater. Trans. A, Phys. Metall. Mater. Sci. 27 (1996) 569–581.
[49] H. Nguyen-Thi, et al., Tailoring of dendritic microstructure in solidification processing by crucible vibration, J. Cryst. Growth 275 (1–2) (2005) e1579–e1584.
[50] E. Liotti, et al., A synchrotron X-ray radiography investigation of induced dendrite fragmentation in Al-15wt%Cu, Mater. Sci. Forum 765 (juill. 2013) 210–214.
[51] H. Nguyen-Thi, et al., In situ and real-time analysis of TEM forces induced by a permanent magnetic field during solidification of Al-4wt%Cu, Mater. Sci. Forum 790–791 (2014) 420–425.
[52] R. Daudin, et al., Particle-induced morphological modification of Al alloy equiaxed dendrites revealed by sub-second in situ microtomography, Acta Mater. 125 (2017) 303–310.
[53] R.H. Mathiesen, et al., X-ray videomicroscopy studies of eutectic Al–Si solidification in Al–Si–Cu, Metall. Mater. Trans. A, Phys. Metall. Mater. Sci. 42 (2011) 170–180.
[54] G. Reinhart, H. Nguyen-Thi, N. Mangelinck-Noel, J. Baruchel, B. Billia, Situ investigation of dendrite deformation during upward solidification of Al-7wt.%Si, JOM 66 (2014) 1408–1414.
[55] J.L. Fife, P.W. Voorhees, The morphological evolution of equiaxed dendritic microstructures during coarsening, Acta Mater. 57 (2009) 2418–2428.
[56] J.L. Fife, M. Rappaz, M. Pistone, T. Celcer, G. Mikuljan, M. Stampanoni, Development of a laser-based heating system for in situ synchrotron-based X-ray tomographic microscopy, J. Synchrotron Radiat. 19 (2012) 352–358.
[57] M.A. Salgado-Ordorica, M. Rappaz, Twinned dendrite growth in binary aluminum alloys, Acta Mater. 56 (2008) 5708–5718.
[58] S.B. Lee, Y.-M. Kim, Direct observation of in-plane ordering in the liquid at a liquid Al/α-Al2O3 interface, Acta Mater. 59 (2011) 1383–1388.
[59] G. Kurtuldu, P. Jarry, M. Rappaz, Influence of Cr on the nucleation of primary Al and formation of twinned dendrites in Al–Zn–Cr alloys: can icosahedral solid clusters play a role?, Acta Mater. 61 (2013) 7098–7108.
[60] M. Rappaz, G. Kurtuldu, Thermodynamic aspects of homogeneous nucleation enhanced by icosahedral short-range order in liquid Fcc-type alloys, JOM 67 (2015) 1812–1820.
[61] M.J. Cooper, The structure of the intermetallic phase θ(Cr–Al), Acta Crystallogr. 13 (1960) 257–263.
[62] H. Tanaka, Bond orientational order in liquids: towards a unified description of water-like anomalies, liquid–liquid transition, glass transition, and crystallization: bond orientational order in liquids, Eur. Phys. J. E 35 (2012).
[63] A. Pasturel, N. Jakse, Influence of Cr on local order and dynamic properties of liquid and undercooled Al–Zn alloys, J. Chem. Phys. 146 (2017) 184502.
[64] A. Pasturel, N. Jakse, Chemically induced structural heterogeneities and their relationship with component dynamics in a binary metallic liquid, Appl. Phys. Lett. 110 (2017) 121902.
[65] D. Turnbull, The 1980 Campbell memorial lecture, Metall. Trans. A 12 (1981).
[66] J. Russo, H. Tanaka, Selection mechanism of polymorphs in the crystal nucleation of the Gaussian core model, Soft Matter 8 (2012) 4206.
[67] M. Asta, et al., Solidification microstructures and solid–state parallels: recent developments, future directions, Acta Mater. 57 (2009) 941–971.
[68] F. Gonzales, M. Rappaz, Dendrite growth directions in aluminum–zinc alloys, Metall. Mater. Trans. A 37 (2006).
[69] S. Henry, Etude de la germination et de la croissance maclées dans les alliages d'aluminium, EPFL, Lausanne, Switzerland, 1999.
[70] M. Bedel, G. Reinhart, C.-A. Gandin, A.-A. Bogno, H. Nguyen-Thi, H. Henein, Evolution of the dendritic morphology with the solidification velocity in rapidly solidified Al-4.5wt.%Cu droplets, IOP Conf. Ser., Mater. Sci. Eng. 84 (2015) 012016.
[71] A. Sémoroz, Experimental Study and Modelling of Nucleation and Growth During Solidification of Al and Zn Coatings, EPFL, Lausanne, Switzerland, 2001.
[72] M.W. Meredith, A.L. Greer, P.V. Evans, The effect of grain refining additions in intermetallic phase selection in dilute Al–Fe alloys, in: SP97, 1997, p. 541.
[73] R.G. Hamerton, H. Cama, M.W. Meredith, Development of the coarse intermetallic particle population in wrought aluminium alloys during ingot casting and thermo-mechanical processing, Mater. Sci. Forum 331 (337) (2000) 143–154.

[74] A. Verma, S. Kumar, P.S. Grant, K.A.Q. O'Reilly, Influence of cooling rate on the Fe intermetallic formation in an AA6063 Al alloy, J. Alloys Compd. 555 (2013) 274–282.
[75] S. Zajac, Effect of Grain Size on AlFeSi Particle Structure and Hot Workability of AA6063 Aluminium Alloy, vol. IM2999, 1993.
[76] S. Zajac, L.O. Gullmann, A. Johansson, B. Bengtsson, Hot ductility of some AlMgSi alloys, Mater. Sci. Forum (1996) 1193–1198.
[77] S. Lu, A. Hellawell, J. Cryst. Growth 73 (1985) 316.
[78] J. Li, et al., The roles of Eu during the growth of eutectic Si in Al–Si alloys, Sci. Rep. 5 (1) (2015).
[79] E. Sarrazin, P. Jarry, Method for Making High Tenacity and High Fatigue Strength Aluminium Alloy Products, EP1766102 (A1), 2005.
[80] S.M. Liang, R. Schmid-Fetzer, Validated thermodynamic prediction of AlP and eutectic (Si) solidification sequence in Al–Si cast alloys, IOP Conf. Ser., Mater. Sci. Eng. 117 (2016) 012003.
[81] T.H. Ludwig, J. Li, P.L. Schaffer, P. Schumacher, L. Arnberg, Refinement of eutectic Si in high purity Al–5Si alloys with combined Ca and P additions, Metall. Mater. Trans. A 46 (2015) 362–376.
[82] M. Zarif, B. Mckay, P. Schumacher, Study of heterogeneous nucleation of eutectic Si in high-purity Al–Si alloys with Sr addition, Metall. Mater. Trans. A 42 (2011) 1684–1691.
[83] J.H. Li, P. Schumacher, Effect of Y addition and cooling rate on refinement of eutectic Si in Al-5 wt-%Si alloys, Int. J. Cast Met. Res. 25 (2012) 347–357.
[84] J.H. Li, S. Suetsugu, Y. Tsunekawa, P. Schumacher, Refinement of eutectic Si phase in Al-5Si alloys with Yb additions, Metall. Mater. Trans. A 44 (2013) 669–681.
[85] P. Srirangam, M.J. Kramer, S. Shankar, Effect of strontium on liquid structure of Al–Si hypoeutectic alloys using high-energy X-ray diffraction, Acta Mater. 59 (2) (2011) 503–513.
[86] D. Granger, Microstructure control in ingots of aluminium alloys with an emphasis on grain refinement, in: Light Metals 1998, 1998.
[87] C.M. Allen, K.A.Q. O'Reilly, P.V. Evans, B. Cantor, The effect of vanadium and grain refiner additions on the nucleation of secondary phases in 1xxx Al alloys, Acta Mater. 47 (1999) 4387–4403.
[88] K. Liu, X. Cao, X.-G. Chen, A new iron-rich intermetallic-Al m Fe phase in Al–4.6Cu–0.5Fe cast alloy, Metall. Mater. Trans. A 43 (2012) 1097–1101.
[89] H. Tezuka, A. Kamio, Influence of minor elements on the crystallization manner of intermetallic phases in unidirectionally solidified AlFe alloys, in: ICAA3, 1992.
[90] P.V. Evans, J. Worth, A. Bosland, S.C. Flood, Intermetallic phase selection in AA1xxx aluminium alloys, in: Solidification Processing SP97, 1997, p. 531.
[91] M.J. Aziz, Model for solute redistribution during rapid solidification, J. Appl. Phys. 53 (1982) 1158–1168.
[92] L. Zhang, E.V. Danilova, I. Steinbach, D. Medvedev, P.K. Galenko, Diffuse-interface modeling of solute trapping in rapid solidification: predictions of the hyperbolic phase-field model and parabolic model with finite interface dissipation, Acta Mater. 61 (2013) 4155–4168.
[93] R. Trivedi, W. Kurz, Dendritic growth, Int. Mater. Rev. 39 (1994) 49–74.
[94] J.Q. Guo, K. Ohtera, K. Kita, T. Shibata, A. Inoue, T. Masumoto, New metastable phases in rapidly solidified Al Zr and Al Ti alloys with high solute contents, Mater. Sci. Eng. A 181–182 (1994) 1397–1404.
[95] C. Colinet, A. Pasturel, Phase stability and electronic structure in ZrAl3 compound, J. Alloys Compd. 319 (2001) 154–161.
[96] A.P. Tsai, Icosahedral clusters, icosaheral order and stability of quasicrystals—a view of metallurgy*, Sci. Technol. Adv. Mater. 9 (2008) 013008.
[97] N. Jakse, A. Pasturel, Liquid aluminum: atomic diffusion and viscosity from ab initio molecular dynamics, Sci. Rep. 3 (2013).
[98] M. Asta, J.J. Hoyt, A. Karma, Calculation of alloy solid–liquid interfacial free energies from atomic-scale simulations, Phys. Rev. B 66 (2002).
[99] S.A. Khairallah, A.T. Anderson, A. Rubenchik, W.E. King, Laser powder-bed fusion additive manufacturing: physics of complex melt flow and formation mechanisms of pores, spatter, and denudation zones, Acta Mater. 108 (2016) 36–45.
[100] U. Scipioni Bertoli, A.J. Wolfer, M.J. Matthews, J.-P.R. Delplanque, J.M. Schoenung, On the limitations of volumetric energy density as a design parameter for selective laser melting, Mater. Des. 113 (2017) 331–340.
[101] A.V. Gusarov, I. Smurov, Modeling the interaction of laser radiation with powder bed at selective laser melting, Phys. Proc. 5 (2010) 381–394.
[102] M.J. Matthews, G. Guss, S.A. Khairallah, A.M. Rubenchik, P.J. Depond, W.E. King, Denudation of metal powder layers in laser powder bed fusion processes, Acta Mater. 114 (2016) 33–42.
[103] C.L.A. Leung, S. Marussi, R.C. Atwood, M. Towrie, P.J. Withers, P.D. Lee, In situ X-ray imaging of defect and molten pool dynamics in laser additive manufacturing, Nat. Commun. 9 (2018).
[104] P. Bidare, I. Bitharas, R.M. Ward, M.M. Attallah, A.J. Moore, Fluid and particle dynamics in laser powder bed fusion, Acta Mater. 142 (2018) 107–120.
[105] T.T. Roehling, et al., Modulating laser intensity profile ellipticity for microstructural control during metal additive manufacturing, Acta Mater. 128 (2017) 197–206.
[106] F. Fetzer, M. Jarwitz, P. Stritt, R. Weber, T. Graf, Fine-tuned remote laser welding of aluminum to copper with local beam oscillation, Phys. Proc. 83 (2016) 455–462.
[107] O. Budenkova, et al., Modelling of Al-7%wtSi-1wt%Fe ternary alloy: application to space experiments with a rotating magnetic field, Mater. Sci. Forum 790–791 (2014).
[108] O. Budenkova, et al., Simulation of a directional solidification of a binary Al-7wt%Si and a ternary alloy Al-7wt%Si-1wt%Fe under the action of a rotating magnetic field, IOP Conf. Ser., Mater. Sci. Eng. 33 (2012) 012046.
[109] X. Mao, H.M. Blackburn, S.J. Sherwin, Nonlinear optimal suppression of vortex shedding from a circular cylinder, J. Fluid Mech. 775 (juill. 2015) 241–265.
[110] U.A. Qadri, G.J. Chandler, M.P. Juniper, Self-sustained hydrodynamic oscillations in lifted jet diffusion flames: origin and control, J. Fluid Mech. 775 (2015) 201–222.
[111] D.G. Eskin, A. Jafari, L. Katgerman, Contribution of forced centreline convection during direct chill casting of round billets to macrosegregation and structure of binary Al–Cu aluminium alloy, Mater. Sci. Technol. 27 (5) (2011) 890–896.
[112] A. Pakanati, K.O. Tveito, M. M'Hamdi, H. Combeau, M. Založnik, Impact of inlet flow on macrosegregation formation accounting for grain motion and morphology evolution in DC casting of aluminium, in: O. Martin (Ed.), Light Metals 2018, Springer International Publishing, Cham, Switzerland, 2018, pp. 1089–1096.
[113] S.R. Wagstaff, A. Allanore, Minimization of macrosegregation in DC cast ingots through jet processing, Metall. Mater. Trans. B 47 (2016) 3132–3138.
[114] S.R. Wagstaff, A. Allanore, Jet mixing in direct-chill casting of aluminum: crater effects and its consequence on centerline segregation, Metall. Mater. Trans. B 48 (2017) 2114–2122.
[115] G.M. Poole, M. Heyen, L. Nastac, N. El-Kaddah, Numerical modeling of macrosegregation in binary alloys solidifying in the presence of electromagnetic stirring, Metall. Mater. Trans. B 45 (2014) 1834.
[116] A.K. Boukellal, J.-M. Debierre, G. Reinhart, H. Nguyen-Thi, Scaling laws governing the growth and interaction of equiaxed Al–Cu dendrites: a study combining experiments with phase-field simulations, Materialia 1 (2018) 62–69.